Surface & Coatings Technology 204 (2009) 336–344

Contents lists available at ScienceDirect

Surface & Coatings Technology

journal homepage: www.elsevier.com/locate/surfcoat

The use of Al–Al_2O_3 cold spray coatings to improve the surface properties of magnesium alloys

K. Spencer [a,b,*], D.M. Fabijanic [c], M.-X. Zhang [a,b]

[a] Division of Materials, School of Engineering, The University of Queensland, St Lucia, QLD, 4072, Australia
[b] ARC Centre of Excellence for Design in Light Metals, Australia
[c] Centre for Material and Fibre Innovation, Deakin University, VIC, 3217, Australia

ARTICLE INFO

Article history:
Received 15 May 2009
Accepted in revised form 24 July 2009
Available online 3 August 2009

JEL classification:
62.20.Qp
81.40.Np
81.40.Pq
81.65.-b
81.65.Kn

Keywords:
Cold spray
Kinetic metallization
Metal matrix composite
Wear
Corrosion

ABSTRACT

Pure Al and 6061 aluminium alloy based Al_2O_3 particle-reinforced composite coatings were produced on AZ91E substrates using cold spray. The strength of the coating/substrate interface in tension was found to be stronger than the coating itself. The coatings have corrosion resistance similar to that of bulk pure aluminium in both salt spray and electrochemical tests. The wear resistance of the coatings is significantly better than that of the AZ91 Mg substrate, but the significant result is that the wear rate of the coatings is several decades lower than that of various bulk Al alloys tested for comparison. The effect of post-spray heat treatment, the volume fraction of Al_2O_3 within the coating and of the type of Al powder used in the coatings on the corrosion and wear resistance was also discussed.

© 2009 Elsevier B.V. All rights reserved.

1. Introduction

The use of magnesium as a lightweight structural material for high volume aerospace/automotive applications is currently a key area of investigation [1,2]. Although in certain applications magnesium alloys have acceptable surface properties [3], the wear and corrosion resistance of magnesium alloys is generally poor [4–6]. There are various surface modification techniques that may improve the surface properties of magnesium alloys [7], but the existing techniques are limited either by performance or cost. While various thermal spray techniques may be used to economically coat magnesium alloys, porosity in the coatings requires some form of post-coating treatment or sealing in order to produce dense coatings that have acceptable corrosion resistance [8–11]. The unsuitable properties as-sprayed limit the potential use of thermal spray coatings on active substrate materials such as magnesium alloys.

The emerging cold spray coating process has potential for use as a simple technique for surface protection of magnesium alloys. In this coating process a metal powder is accelerated in a gas stream toward a metal substrate at velocities of 500–1000 m s^{-1}, producing a metallurgical bond with the metal substrate on impact [12,13]. Although cold spray coating technology is often discussed in the context of improving surface properties, its application on Mg alloys has not been well studied. Cold spray composite coatings of Al–Al_2O_3 [14], Al–SiC [15] and Al–TiN [16] on Al substrates have been studied and the corrosion behaviour of the coatings is reported to be similar to that of the substrate. However, Spencer and Zhang's previous work [17] has shown that if cold sprayed Al coatings on Mg alloy substrates are not sufficiently dense, the rate of corrosion when immersed in a solution of 5% NaCl is accelerated when compared to the substrate alone, due to galvanic coupling. Therefore, reduction of porosity of the sprayed coatings plays a key role in improvement of the corrosion resistance of the coatings. It is known that the addition of hard ceramic particles into cold sprayed coatings not only improves the hardness and wear resistance, but also increases the density of the coatings [14,18]. Coatings with improved density have the potential to improve the corrosion resistance due to reduced porosity, provided there is no galvanic coupling between the ceramic particle and the coating matrix material. The present work is a comprehensive investigation of the microstructure, wear resistance and corrosion resistance of Al–Al_2O_3 composite coatings on AZ91E Mg alloy substrates

* Corresponding author. Division of Materials, School of Engineering, The University of Queensland, St Lucia, QLD, 4072, Australia. Tel.: +61 7 3365 3580; fax: +61 7 3346 7015.
E-mail address: k.spencer@uq.edu.au (K. Spencer).

0257-8972/$ – see front matter © 2009 Elsevier B.V. All rights reserved.
doi:10.1016/j.surfcoat.2009.07.032

produced using cold spray. The results will be quantitatively compared with those of both AZ91E substrate and bulk Al alloy. Bulk Al alloys are used as a reference for comparison since magnesium is being considered as an alternative to aluminium alloys in many light weighting applications [19].

2. Experimental methods

The substrate material used was a cast AZ91E alloy, solution treated at 413 °C for 6 h and aged at 168 °C for 18 h. It was prepared for cold spray by grinding with 1200 grit SiC paper and cleaning with ethanol. Spherical commercial purity Al and 6061Al alloy powders with average an average particle size of 15 μm and 22 μm respectively were used as the matrix material in the powder mixtures. The reinforcement used was α-Al_2O_3 powder with an average particle size of 20 μm. The Al_2O_3 was mixed with the Al powders in a Turbula mixer, and mixtures of 25, 50 and 75 vol.% Al_2O_3 were prepared. The composition of the Al powders and the AZ91E substrate material is given in Table 1. The composition of the powders was supplied by the manufacturers, and that of the substrate was obtained using inductively coupled plasma atomic emission spectroscopy (ICP-AES).

The cold spray coating was produced using a Kinetic Metallization (KM) system, which is a commercially-available cold spray variant (Inovati, Santa Barbara, CA, USA). Whereas most cold spray systems use a de Laval convergent–divergent nozzle to accelerate the process gas to supersonic speeds [20], KM uses a convergent nozzle to accelerate the process gas to ~Mach 1 [21]; for the process conditions used in the present work, that equates to a gas speed of 1020 m/s. In order to increase the impact velocity helium was used as the carrying gas, with a driving pressure of 620 kPa. The temperature of the mixing chamber, which is close to the temperature of the powder/gas mixture prior to accelerating through the nozzle throat, was 125 °C. The mass flow rate of the powder mixtures injected into the gas stream was 15 g min^{-1}. The nozzle standoff distance from the substrate was 12 mm and the traverse speed was 50 mm min^{-1}. Pure Al cold spray coatings were tested for corrosion and wear in both the as-sprayed condition, and after a post-spray heat treatment of 400 °C for 2 h in an argon atmosphere. The 6061Al coatings were only tested in the as-sprayed condition.

Corrosion resistance of the coatings was assessed visually using salt spray testing, and electrochemically using linear potentiodynamic polarisation, both in a neutral 5% NaCl solution. The salt spray tests were conducted as per the ASTM B117 standard. For all corrosion tests only the cold spray coating surface was exposed to the electrolyte, ground to a 1200 grit finish; any uncoated substrate material was masked off using an epoxy resin. For the polarisation tests, electrical contact was made via a sheathed copper wire drilled into the AZ91E substrate, sealed with epoxy along with any exposed substrate. The samples were cathodically polarised approximately 2 V below the open circuit potential. This was necessary in order to dissolve the existing passive layer so that its formation and potential range could be observed [22]. Only the anodic branch is shown in the results, and the scan rate used was 0.166 mV s^{-1}.

Table 1
Composition of commercial purity Al and 6061Al powder as supplied by the manufacturers, and composition of the AZ91E substrate material obtained by ICP-AES.

Material	Pure Al powder	6061Al powder	AZ91E substrate
Al	Balance	Balance	8.3
Mg	0.001	1.0	Balance
Si	0.011	0.5	0.01
Zn	0.002	N/A	0.52
Cu	<0.001	0.25	<0.005
Fe	0.023	0.25	<0.005
Ni	0.001	N/A	<0.005

Values are in wt.%.

Samples were prepared metallographically as follows, using an automatic polishing machine. They were ground using wet SiC paper in successively finer grades, finishing with 4000 grit paper. Polishing was done using 6 μm diamond paste with a nylon weave cloth, and then using 1 μm diamond paste with a soft nap cloth. This approach was used to minimise rounding of the coating/substrate interface due to the higher hardness of the coating. Greyscale thresholding and image binarisation were used to estimate the porosity of the Al and 6061Al coatings; this technique was not suitable for use with coatings containing Al_2O_3 due to insufficient contrast between fine Al_2O_3 particles and pores in the coating. Identification of intermetallic phases in heat treated samples was done using a combination of Energy Dispersive X-ray analysis and by X-ray diffraction (XRD), and is detailed elsewhere [23].

Microhardness testing was carried out using a load of 200 g on polished coating cross-sections at a series of random points, with care taken to avoid measuring too close to the coating surface or coating/substrate interface. These tests were repeated using a Vickers hardness tester with a 5 kg load. Wear tests were performed using a ball-on-disc tribometer. Cold spray disc samples with a 19 mm diameter were used, with the surface polished flat to a 1 μm finish. A load of 3 N was used, with a linear speed of 20 cm s^{-1}. Three (3) tests of each material were conducted over a wear length of 500 m and the counter material was a 6 mm ball made of 52,100/100Cr6 bearing steel (800 $HV_{5\ kg}$, 64 HR_C). Wear scar profiles were measured radially from the centre of the disc using a stylus profilometer with a 0.5 μm step size; twelve (12) wear scar profiles were used to determine an average wear area and subsequent wear rate. Wear and corrosion tests were also conducted on various bulk materials for comparison. The bulk alloys used for comparison were commercial purity Al, Al–12%Si, 356.0 Al (Al–7%Si–0.4%Mg), and commercial purity Mg, AZ91E, and ZE41A magnesium alloys.

Tensile bond strength testing was done following the ASTM standard C633-01, with increased sample length as suggested by Han et al. in order to ensure pure tensile loading of the coating [24]. The coatings were sprayed on the end face of AZ91 T6 substrate lugs 50.8 mm long × 25.4 mm dia., and the samples were glued to the test fixture using HTK Ultra Bond 100 epoxy, cured at 150 °C for 90 min. Three samples were tested and the average result was taken for each condition.

The volume fractions of Al and Al_2O_3 in the sprayed coatings was measured using least squares full profile fitting and integration of the XRD spectra, with the fitting performed using pseudo-Voigt peak shape functions [25,26]. The technique was verified using the source powder mixtures of known composition, with the error less than 1 vol.%. The error bars shown in all results in this paper represent one standard deviation from the mean.

3. Results and discussion

3.1. Coating microstructure

The general microstructure of the 6061Al coatings on an AZ91E substrate is shown in Fig. 1 for a 6061Al coating (a), and coatings deposited using powder mixtures of 25 vol.% Al_2O_3 (b), with the Al_2O_3 indicated, and 75 vol.% Al_2O_3 (c). Some porosity can be observed within the 6061Al coating, estimated to be 1 to 1.5 vol.% as measured by image analysis; in the case of the coatings containing Al_2O_3 it was not possible to obtain a clear estimate. The coatings containing Al_2O_3 show a uniform dispersion of both Al and Al_2O_3 particles, which suggests that under the spray conditions used the two species did not separate in the gas flow stream. Fig. 2 shows the interface between the substrate and the 6061 alloy and 6061–50% Al_2O_3 coatings. Since the substrate is a relatively soft Mg alloy there is a significant amount of deformation of the substrate by the impacting Al particles Fig. 2(a). The interface between the coating and the substrate is relatively flat in all cases, and no mutual penetration is observed on a macroscopic scale.

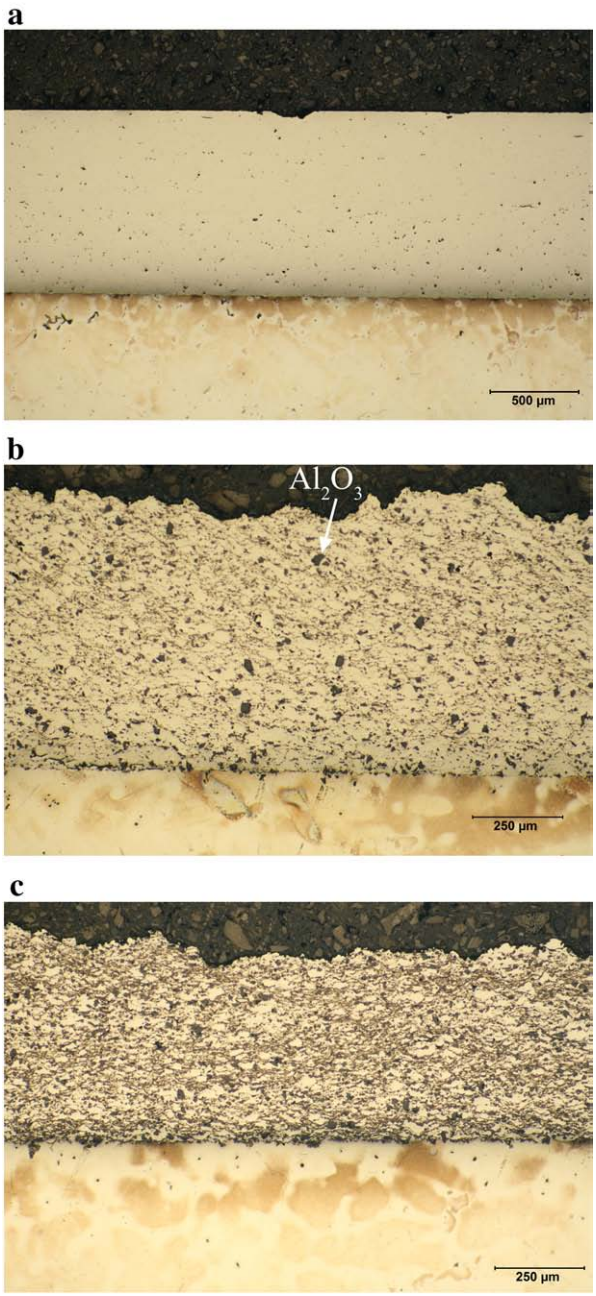

Fig. 1. (a) Optical micrograph of 6061Al KM coating on an AZ91 substrate, as-sprayed. (b) Optical micrograph of 6061Al–25% Al_2O_3 KM coating on an AZ91 substrate, as-sprayed. The black phase is the Al_2O_3. (c) Optical micrograph of 6061Al–75% Al_2O_3 KM coating on an AZ91 substrate, as-sprayed. The black phase is the Al_2O_3.

The structure of the coating interface is shown after a post-spray heat treatment of 400 °C for 2 h in Fig. 2(c) and (d). A 20–30 μm thick diffusion layer has formed at the interface comprising mostly $Mg_{17}Al_{12}$, with a thin and discontinuous layer of Al_3Mg_2 in both types of coatings. The characterisation of these layers and the details of their formation are discussed elsewhere [23]. Some cracking of the intermetallic layers is evident; it is suspected that this occurs during cooling from the heat treatment temperature because cracking is not observed when the layers grow thicker than 100 μm [23]. Beyond the growth of these diffusion layers there were no notable changes in the coating microstructure. The growth of these diffusion layers confirms there is a clean metallic bond at the interface. This suggests that any surface oxide present on the particles was broken sufficiently during the impact process to enable chemical diffusion to occur across the interface.

3.2. Relative deposition efficiency

The actual volume fraction of Al_2O_3 in the cold sprayed coating is normally lower than that in the source powder mixture prepared for spraying. The deposition efficiency is defined as the percentage of the powder that was actually deposited in the coating. As the deposition efficiency depends on a number of variables such as the temperature, flow rate, carrying gas pressure etc., the absolute deposition efficiency of the powder mixtures was not measured. However, for a specified spray condition a qualitative measure of the deposition efficiency of different Al–Al_2O_3 mixtures may be inferred from relative coating thickness. Furthermore, the *relative* deposition efficiency of the Al and Al_2O_3 can be calculated by comparing the volume fraction of Al and Al_2O_3 in the source powder to that in the deposited coatings. Using this idea the relative deposition efficiency of the Al_2O_3 powder is plotted in Fig. 3. The dashed line represents the condition where both the Al and Al_2O_3 powders deposit in the same proportion as in the source powder. The compositions falling below this line indicate that the volume fraction of Al_2O_3 in the sprayed coating is lower than that in the source powder mixture. Put another way, the relative deposition efficiency of the Al_2O_3 powder is lower than that of the Al powder. Fig. 3 shows that as more Al_2O_3 is added to the source powder mixture, the relative deposition efficiency of Al_2O_3 decreases.

With regard to the overall deposition efficiency of the Al–Al_2O_3 mixtures, it was observed that using the same spray conditions the thickest coatings were obtained with the Al–25%Al_2O_3 mixtures. Increasing the Al_2O_3 content beyond this level resulted in a subsequent reduction in deposition efficiency. The increased overall deposition efficiency realised by adding a smaller amount of Al_2O_3 to the source powder mixture is likely due to a combination of some anchoring of the Al_2O_3 particles during the coating process, and the forced compatibility of the relatively soft Al particles deforming around the harder Al_2O_3 particles.

The loss of Al_2O_3 during the coating process can be explained by the fact that Al_2O_3 cannot form a bond with itself, and can deposit onto the substrate in a monolayer at most. Unless an Al_2O_3 particle is trapped between adjacent Al particles it will simply rebound from the coating, especially since the bulk modulus of the Al_2O_3 particles is roughly 3–5 times that of the Al powder. This is why the proportion of Al_2O_3 is lower in the sprayed coating than in the source powder. As the proportion of Al_2O_3 in the powder mixture is raised, increased interaction between Al_2O_3 particles will cause even more of them to be rebounded, reducing both the overall deposition efficiency and the relative deposition of the Al_2O_3 compared to the Al. For convenience, the samples will be referred to by their source powder compositions instead of the deposited ones.

3.3. Bond strength

Table 2 lists the results of the tensile bond strength measurements performed on selected coatings. In all cases the failure mode was cohesive, roughly through the coating mid-plane. This means the strength of the interface is greater than that of the coating itself. In service the coatings should be very stable against spalling, as it was possible to grind through the coating down to the substrate without any spalling observed.

The strength of the coatings without any Al_2O_3 was lower than those with added Al_2O_3. Beyond that, the tensile bond strength of the coatings was approximately independent of the Al_2O_3 content. It is likely the forced compatibility of plastic deformation caused by the Al_2O_3 that leads to internal strengthening of the coating. It is expected that beyond a critical volume fraction of Al_2O_3 within the coating that the loss of metallically bonded area would offset any strength gain of the coating, and the failure mode would become an adhesive failure at the interface. This was not observed in the present work, as the maximum amount of Al_2O_3 deposited was only ~28 vol.%.

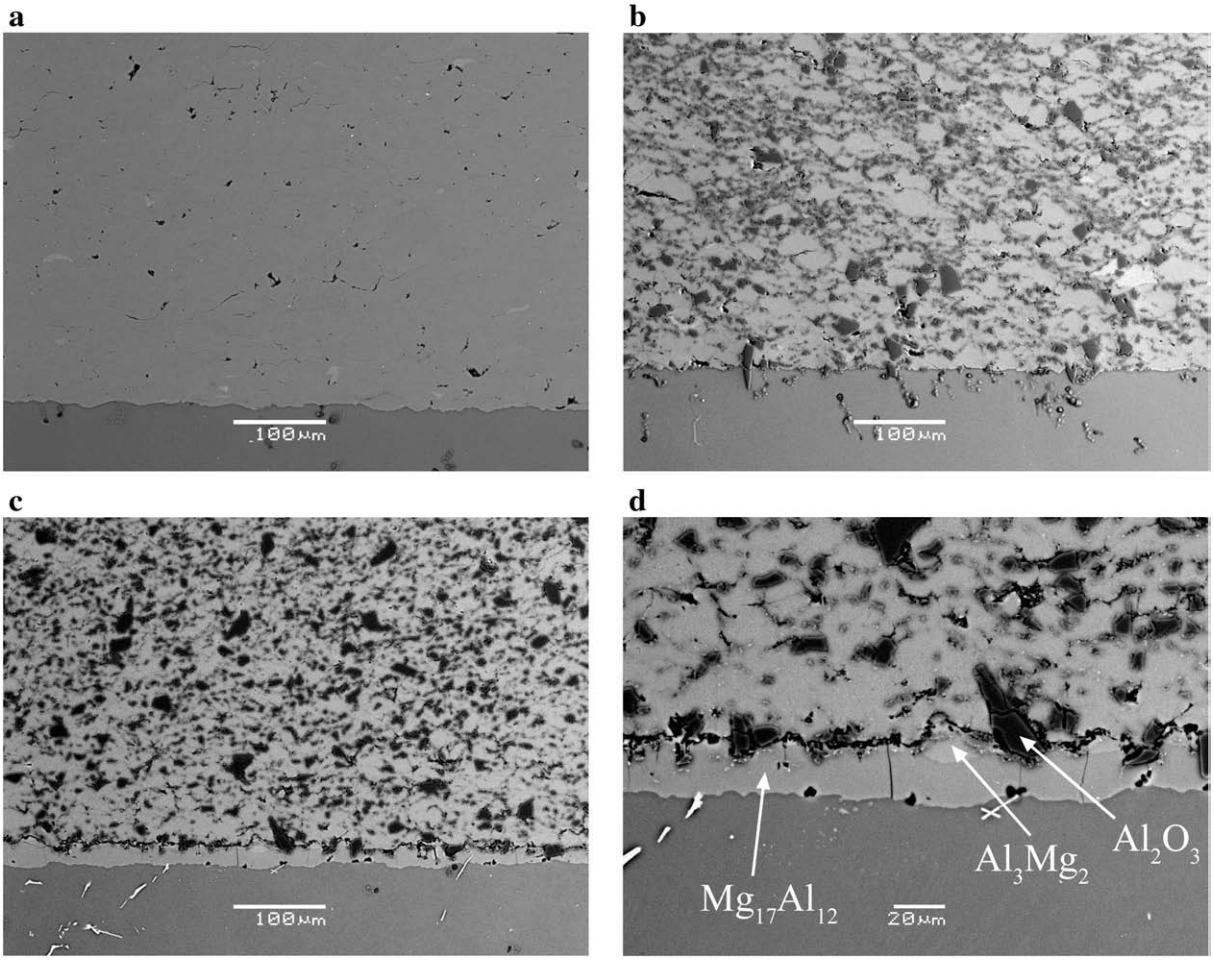

Fig. 2. Backscatter electron micrographs of the coating/substrate interface; substrate material is AZ91E magnesium alloy. (a) Unmixed 6061Al coating. (b) 6061Al–50% Al_2O_3 coating. (c) 6061Al–50% Al_2O_3 coating after heat treatment of 400 °C for 2 h. (d) Enlarged view of coating/substrate interface in (c).

3.4. Corrosion behaviour of the coatings

3.4.1. Salt spray testing

The major experimental difficulty when performing the salt spray tests was to prevent any contact between the electrolyte and the uncoated substrate. Although epoxy was used to mask the substrate, swelling of the epoxy due to moisture absorption allows the salt to penetrate to regions of uncoated substrate. In these cases the preferential attack of the substrate and the formation of a low density corrosion product on the substrate surface forcibly removed the coatings on the as-sprayed samples. However, this problem occurred less frequently in the post-spray heat treated samples. There are three possible reasons for this: (1) The growth of the diffusion layer forms a barrier to electrolyte penetration at the edge of the sample where the epoxy has expanded; (2) The formation of the diffusion layer increases the strength of the bond at the interface, making delamination more difficult, and/or (3) The annealing process has relaxed the compressive stress that builds up at the coating interface during spraying, again making delamination more unlikely. Therefore, only the salt spray results for heat treated sample are reported in the present work, even though the removed coatings of the as-sprayed samples often remained fully intact. Fig. 4 shows the macrographs of the sample surfaces before and after a 10 day neutral salt spray

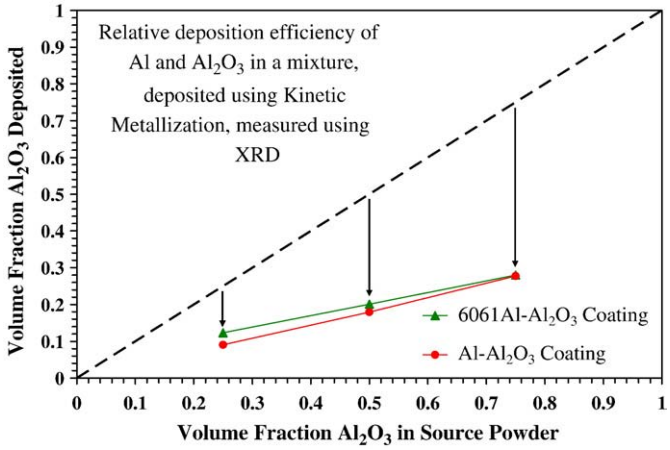

Fig. 3. Volume fraction of Al_2O_3 deposited in the coatings as compared to the source powder mixture.

Table 2
Results of bond strength measurements of selected coatings, using AZ91E substrate material in the T6 temper.

Material	Bond strength (MPa)	Failure mode
Al	30.0 ± 2.7	Cohesive
Al–25% Al_2O_3	41.4 ± 3.6	Cohesive
6061Al	36.2 ± 2.9	Cohesive
6061Al–25% Al_2O_3	40.4 ± 3.1	Cohesive
6061Al–75% Al_2O_3	42.0 ± 0.2	Cohesive

Error is one standard deviation.

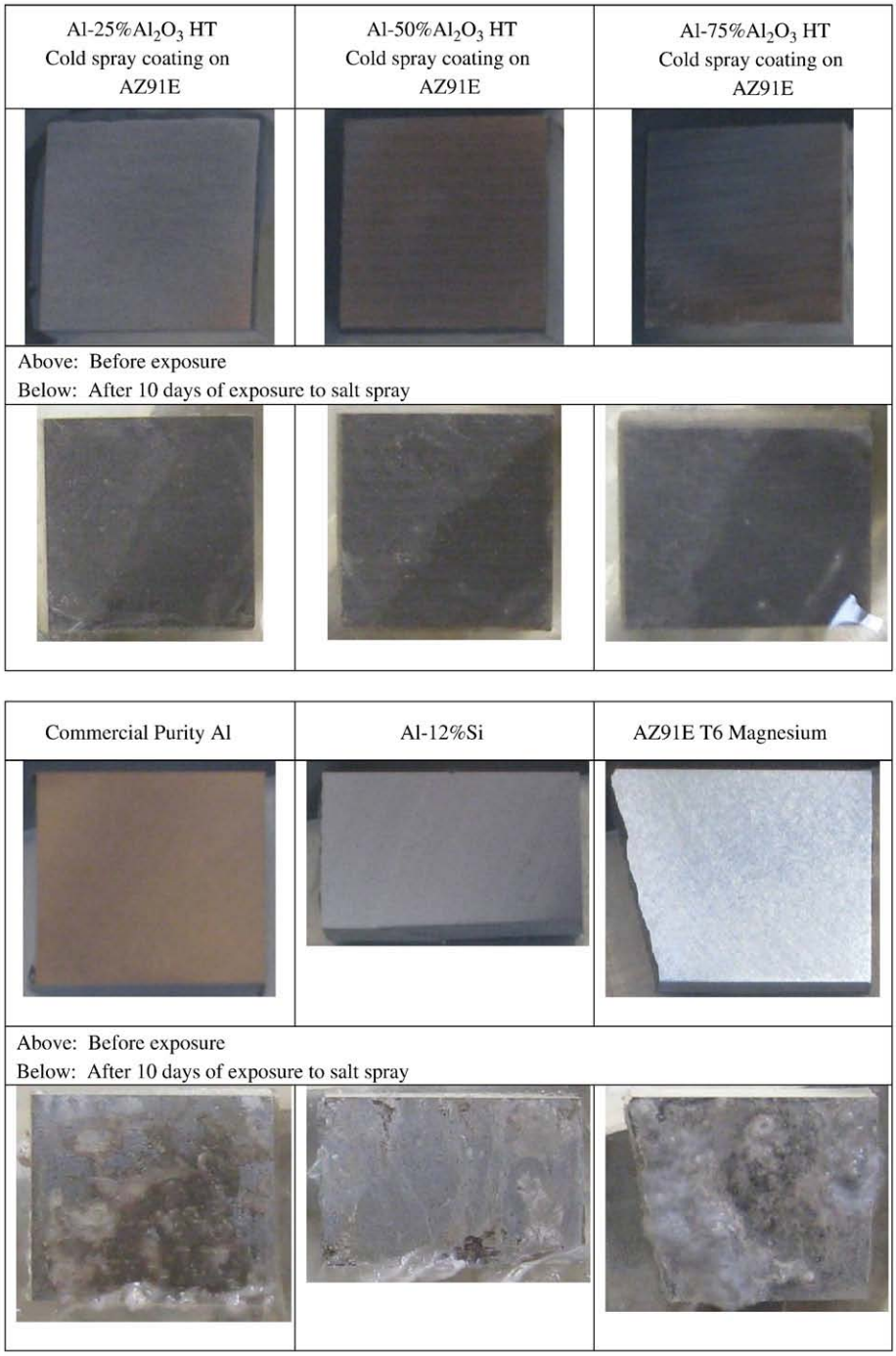

Fig. 4. Cold spray coating and bulk test samples before and after a 10 day salt spray exposure. "HT" in the cold spray coatings denotes a heat treatment of 400 °C for 2 h.

exposure, comparing the heat treated cold sprayed coatings to pure Al, Al–12%Si and the AZ91E substrate material. The cold spray coatings have a similar level of surface attack to pure Al after the salt spray exposure, while the AZ91E substrate is visibly more attacked. This implies that the corrosion resistance of the Al cold spray coatings in a salt spray test is similar to that of the bulk Al alloys tested. A heat treatment is not necessary, but does increase the protective nature of the coatings if any electrolyte is allowed to penetrate to the coating/substrate interface.

3.4.2. Electrochemical corrosion testing

The response of the coatings subject to linear polarisation is shown in Fig. 5, plotted with respect to the standard hydrogen electrode (SHE) potential. The response of the as-sprayed Al and Al–Al_2O_3 cold spray coatings is shown in Fig. 5(a). It can be seen that the volume fraction of Al_2O_3 has no significant effect on the polarisation behaviour. The corrosion current density is roughly the same in each case, as is the pitting potential, where the behaviour transitions from passive to stable pitting; the passivation potential range and the potential above which pitting occurs are indicated in the figure. Of interest is the "noise" in the passive region of the polarisation curves, which is interpreted physically as the formation of metastable pits that are subsequently repassivated [27]. A comparison of the polarisation response of the coatings with bulk commercial purity Al and the AZ91E substrate material shows that the polarisation behaviour of the coating is similar to that of the bulk Al alloys;

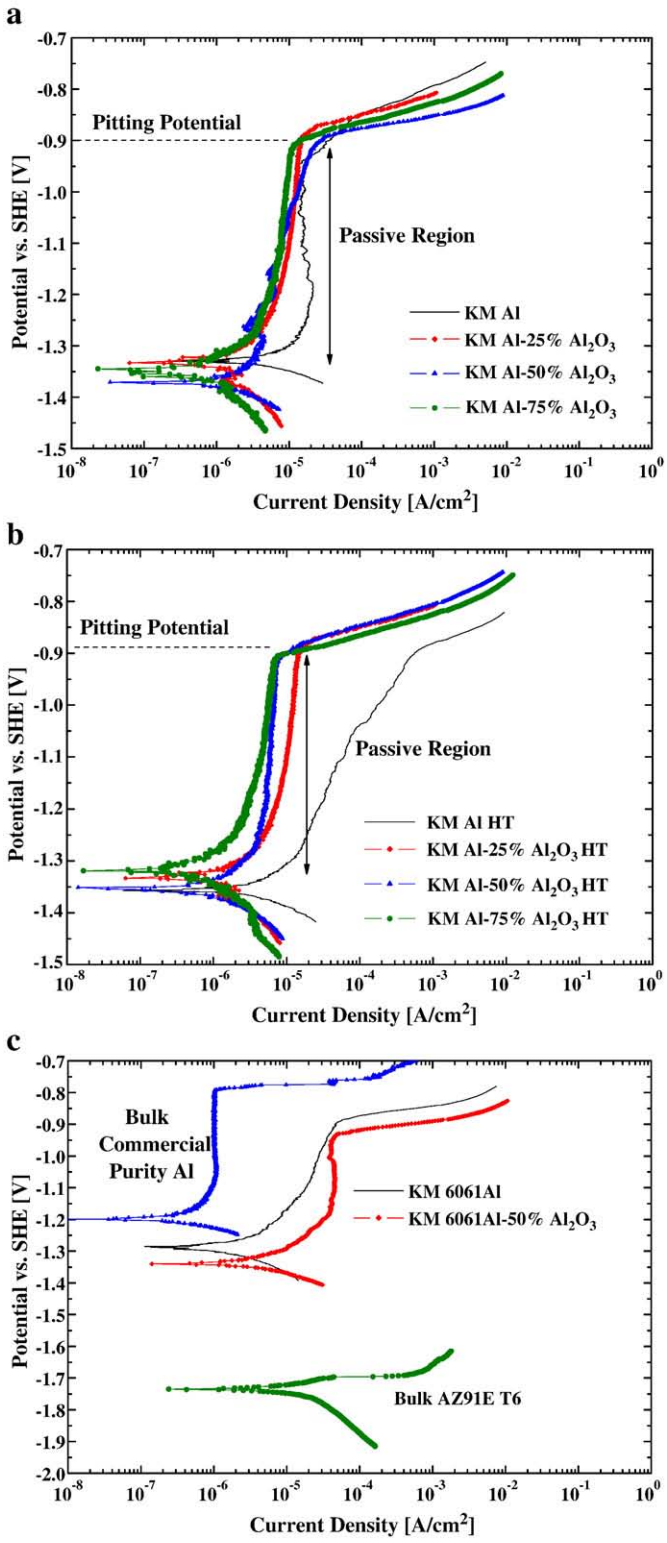

Fig. 5. (a) Linear polarisation behaviour of Al coatings, as-sprayed. (b) Linear polarisation behaviour of Al coatings, after a heat treatment of 400 °C for 2 h. (c) Linear polarisation behaviour of 6061Al coatings as–sprayed, compared to bulk Al and AZ91E T6.

however, the AZ91E substrate has a much more active corrosion potential. This is consistent with the results of the salt spray testing.

The effect of the post-spray heat treatment of 400 °C for 2 h on the polarisation response of the cold spray coatings is shown in Fig. 5(b). The corrosion potential is the same for all of the samples tested, and is similar to the lowest value observed for the as-sprayed samples. The smooth character of the curves in the passive region suggests there is much less metastable pit formation below the pitting potential. The transition from passive to pitting behaviour is also much more abrupt than in the as-sprayed samples, although the pitting potentials are the same in both cases. Therefore, while the overall electrochemical behaviour is unchanged as a result of the heat treatment, stability against the formation of metastable pits has increased, and the corrosion potential is more reproducible. There are several possible reasons for this: (1) Diffusion across particle boundaries similar to that in sintering has increased the electrical conductivity of the coating. This has been observed in the case of annealed copper coatings where an annealing treatment restored the electrical conductivity of cold sprayed Cu coatings to that of bulk annealed Cu [28,29]; (2) Diffusion across the coating/substrate interface has reduced the contact resistance; and (3) The reduction in dislocation density in the coatings from the annealing treatment reduced the tendency to form pits. The polarisation behaviour of the 6061Al coatings is shown in Fig. 5(c) and is very similar to that of the pure Al coatings.

The effect of a post-spray heat treatment on the properties of cold spray coatings has been examined by a number of authors [28–35]. In general a post-spray annealing treatment reduces the hardness of the coatings due to annealing, and increases ductility in tension; both of these results are as expected. The effect of post-spray annealing on other properties such as electrical resistivity and elastic modulus is not as clear. This may be related to how close the behaviour of the cold sprayed deposit is to that of the equivalent bulk material; in some cases the electrical resistivity [29] and elastic modulus [33] of the coating are similar to those of equivalent bulk material, while in other cases the cold spray deposit has significantly different properties [31]. Comparison of the fracture behaviour of cold spray coatings before and after heat treatment suggests that heat treatment does indeed result in significant sintering of the coating [30]. As just one example, varying the particle size for the same coating material can have intrinsic effects such as increased interface per unit volume, in addition to extrinsic effects such as increased interface oxidation for smaller particle sizes. Both of these can affect both electrical resistivity and the elastic modulus. More investigation is required to understand the relationship between cold spray deposits and bulk material, and also the effect of a post-spray heat treatment.

For comparison with the cold spray coatings, the polarisation curves of the AZ91E substrate material and the commercial purity bulk Al are shown. The cold spray coatings show similar behaviour to that of the bulk Al, and much better corrosion resistance than the AZ91E substrate material.

In summary, the electrochemical behaviour of the cold spray coatings is similar to that of a bulk Al alloy in a 5% neutral NaCl solution. Compared to the AZ91E substrate on which the coatings were deposited, the coatings exhibit significantly improved corrosion resistance in this environment as they passivate and have a higher pitting potential. Performing a post-spray heat treatment on the coatings does not significantly affect their performance under these conditions.

3.5. Microhardness and wear resistance

Fig. 6 shows the microhardness data for the cold spray coatings as a function of Al_2O_3 content. With increasing additions of Al_2O_3 to the Al and 6061Al coatings there is a moderate increase in microhardness. This is true for both the as-sprayed and heat treated coatings. Hardness tests were also repeated using a 5 kg load and a larger indenter, with the same results obtained. The decrease in hardness after post-spray heat treatment is a result of the impact-induced cold work in the coating being annealed.

In contrast to the microhardness data, increasing additions of Al_2O_3 had a significant effect on the wear resistance as shown in Fig. 7. The wear rate of the Al–25% Al_2O_3 and 50% Al_2O_3 composite coatings is

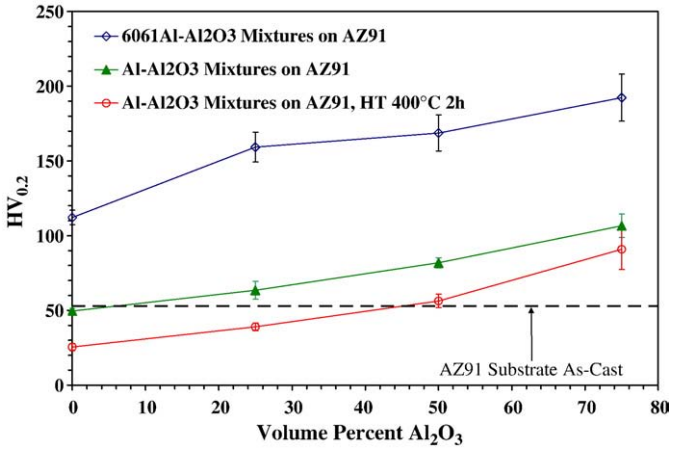

Fig. 6. Vickers microhardness of cold spray as a function of Al_2O_3 content.

reduced by roughly two decades compared with the pure Al coating. The latter has very close wear rate to the bulk AZ91E T6 alloy, the 356.0 Al alloy and the Al–12 wt.%Si alloy under the present testing conditions. With the addition of 75% Al_2O_3 the wear rate decreases by over five decades.

A typical wear track from a pure Al cold spray coating is shown in Fig. 8(a). The smeared appearance of the surface is typical of adhesive wear, and the wear track profiles show evidence of ploughing and extrusion of the worn material outside the wear track. The loose wear debris had the same colour and appearance of the coating material, again suggesting an adhesive wear mode. Further evidence of adhesive wear is seen by examining the worn counter material (not shown here). The Al has adhered to the surface of the steel counter pin, and the counter pin appears to be virtually unworn. This is a case of adhesive material transfer from the softer coating to the harder counter material. Fig. 8(b) shows a wear track from an Al–50% Al_2O_3 coating, which is also typical of the wear tracks from Al–25% Al_2O_3 coatings. The appearance of the track shows signs of smearing and adhesive wear as in the pure Al coatings, but there is also some evidence of abrasive wear. The wear debris was a mixture of light coloured material similar to that of the coating, but also dark debris suggesting some oxidation of the wear debris. The steel counter pin was worn partially flat and there was some Al adhered to the surface. The worn surface of an Al–75% Al_2O_3 coating is shown in Fig. 8(c). The regular markings and lack of smearing are characteristic of abrasive wear. The wear debris was mostly dark in colour, and the steel counter pin was worn completely flat. The wear behaviour can therefore be summarised as a transition from adhesive to abrasive wear with

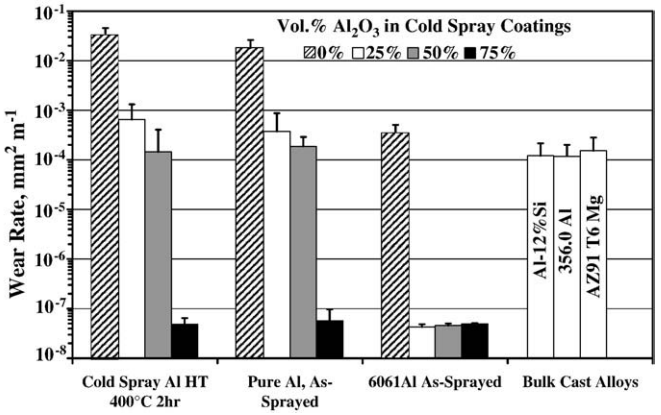

Fig. 7. Wear volume per unit wear distance of coatings compared to bulk alloys.

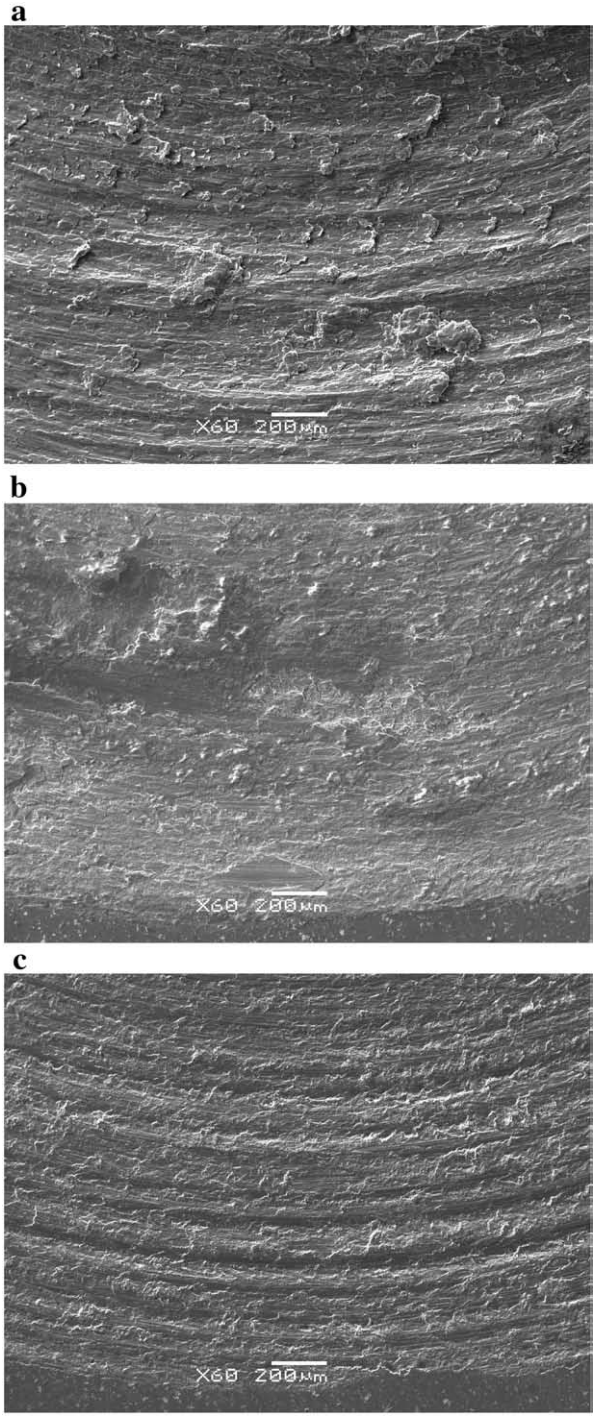

Fig. 8. (a) Scanning electron micrograph of the wear track on a cold sprayed Al coating. (b) Scanning electron micrograph of the wear track on a cold sprayed Al–50% Al_2O_3 coating. (c) Scanning electron micrograph of the wear track on a cold sprayed Al–75% Al_2O_3 coating.

increasing Al_2O_3 additions. This transition is reflected by a significant reduction in wear rate of the coatings.

There was no significant difference in the wear rate between the as-sprayed coatings and the coatings that were heat treated at 400 °C for 2 h, despite the reduction in hardness resulting from the heat treatment. The appearance of the wear tracks and also the wear debris was the same in both cases. This suggests that at least in the case of pure Al which is very soft, it is the Al_2O_3 content that determines the wear behaviour and not the state of the Al matrix material. Replacing pure Al with 6061Al as the matrix material leads to a similar transition in wear

behaviour as the Al_2O_3 content is increased in the source powder; however, this transition occurs with only 25 vol.% Al_2O_3 in the source powder (~12% deposited). Increasing the Al_2O_3 content beyond this level did not lead to any further drop in the wear rate in the 6061Al coatings. This implies that in 6061Al coatings the higher strength of the matrix material enables a transition from adhesive to abrasive wear with a smaller fraction of Al_2O_3 in the coating. The lower wear reduction efficiency of the Al_2O_3 in the pure Al matrix vs. in the 6061 alloy may be related to easier pull-out of the Al_2O_3 particles in the softer pure Al matrix. As this mechanism was not investigated in detail it will not be discussed further. It should be emphasised that the effect of load and speed was not examined, and the load used represents a relatively low load as it was more important to increase the wear distance in the present work.

In general it can be stated there is a critical volume fraction of Al_2O_3 within the composite coating where a transition from adhesive to abrasive wear occurs under the present test conditions. Given the change in wear mechanism, it is not surprising that in this case the microhardness is a poor predictor of wear resistance. In the case of Al-MMCs, it has been observed that there is not a unique relationship between hardness and tensile strength [36]. This has been attributed to the insensitivity of the hardness test to cracking of the reinforcement particles, as the state of stress in a hardness test is dominated by hydrostatic compression, which greatly suppresses damage accumulation [37,38]. Plastic deformation in uniaxial tension, on the other hand, promotes damage accumulation. It is clear that caution is required when using hardness to predict mechanical behaviour of non-monolithic materials. In the case of wear, deformation is primarily by shear and comparison of this to a hardness test dominated by hydrostatic compression will have similar limitations.

Fig. 9 is a plot of the standard deviation of the wear rate from Fig. 7 against the wear rate. It illustrates that increasing additions of Al_2O_3 reduce the standard deviation of the wear rate, roughly in proportion to the reduction in wear rate itself. This implies that adding Al_2O_3 to the coating not only reduces the wear rate, but the wear rate also becomes more stable.

Another assessment of the stability of wear is behaviour of the friction coefficient during the wear test, shown in Fig. 10. The friction coefficient for the 6061Al is very unstable, with most of the sharp deviations in the upward direction. This is indicative of stick-slip behaviour with periodic transfer of material from the coating to the steel counter pin. Such periodicity is also evident in the breaks in the smeared wear track in Fig. 8(a). The reduction in the friction coefficient is typical of run-in during a wear test where the same surface is re-traversed by the counter material [39].

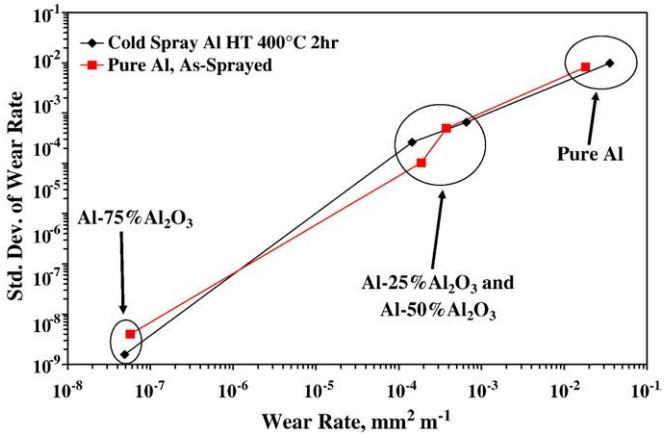

Fig. 9. Standard deviation of wear rate plotted against wear rate, for the Al-MMC coatings.

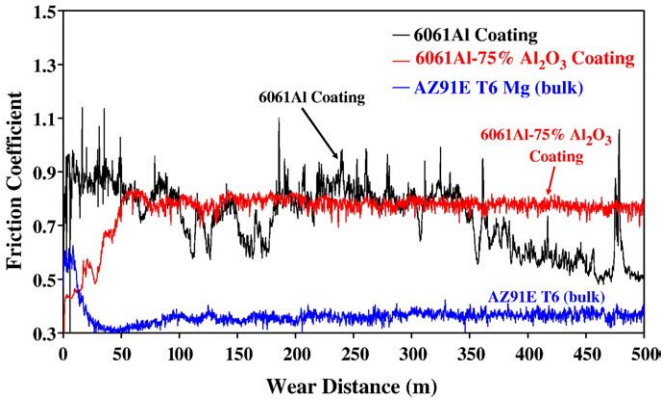

Fig. 10. Friction coefficient vs. sliding wear distance for select materials.

The friction behaviour of the of the 6061Al–75%Al_2O_3 in Fig. 10 is significantly different from that of the unreinforced coating. This is the simplest case of run-in behaviour, where the friction coefficient rises monotonically to a steady state value. This run-in is likely a transition from adhesive wear of the surface to a state of 3-body abrasive wear as the Al_2O_3 is released from the 6061Al matrix. Similar friction behaviour has been observed in particle-reinforced 6061Al previously [40,41]. It has also been observed in the case of Al_2O_3 reinforced 6061Al that the wear resistance is very high under small applied loads, where the Al_2O_3 particles are able to support the load above the metal matrix [42]. This is only possible with relatively large Al_2O_3 particles as used in the present work.

The Al_2O_3 reinforced Al coatings have a higher friction coefficient than the unreinforced coatings, but the wear rate of the reinforced coatings is much lower. In the case of the unreinforced coatings, the friction coefficient is dominated by the yield stress in shear of the Al, since this is a case of adhesive transfer. The situation is very different in the case of the particle-reinforced coatings, where the steel counter pin was ground flat. In this case the Al_2O_3 is deforming the steel counter pin in shear during the wear process; the higher yield strength of the steel in shear is expected to lead to a higher friction coefficient. The overall wear behaviour may be simplified by concluding that the addition of Al_2O_3 to the Al cold spray coatings transfers wear from the coating to the steel counter pin.

The friction behaviour of the AZ91 Mg shows a much faster run-in than in the case of the Al coatings. The AZ91 has both a lower friction coefficient and a lower wear rate than the unreinforced Al coatings. The explanation is not obvious and merits some discussion. It has been suggested that the coefficient of friction between two metals is related to their mutual solubility, and metals with little or no mutual solubility have a low coefficient of friction [43,44]. This view is controversial, and it has been argued that bulk equilibrium properties cannot be used to determine behaviour on the surface layer of materials [45]. A more qualitative but satisfactory explanation is that metals with a hexagonal crystal structure generally have lower friction coefficients and smaller rates of wear than metals with a cubic structure, of roughly comparable strength [46]. This is true particularly in the case of hexagonal metals that deform mainly be basal slip, such as AZ91 Mg deformed near room temperature [47]. A simple explanation is that basal glide alone (with or without twinning) cannot accommodate bulk deformation sufficiently to provide the same level of conformal contact that is possible with contacting cubic metals, which have more operative slip systems [44]. This point is illustrated in the wear data of Chen and Alpas for AZ91 Mg [48], who used the same steel counter material as in the present work. They observed that above a certain temperature, the wear rate sharply transitioned from mild to severe. This transition is likely related to the operation of additional slip modes in the AZ91 Mg at higher temperatures [47]. An extreme case of this argument is observed in the case of cobalt, which undergoes a transition from hexagonal to face-centre cubic. At the temperature where

cobalt transforms from hexagonal to face-centre cubic the coefficient of friction sharply increases [49].

4. Summary and conclusions

1. The addition of Al_2O_3 to Al-based cold spray coatings increases the tensile bond strength.
2. The corrosion resistance of the Al–Al_2O_3 composite coatings was similar to that of bulk Al alloys, and significantly better than the AZ91E Mg substrate. Neither the Al_2O_3 content of the coating nor a post-spray heat treatment had any significant effect on the polarisation behaviour of the coatings. Post-spray heat treatment did improve the resistance to coating delamination where substrate attack was allowed to occur during salt spray testing.
3. Although the addition of Al_2O_3 to pure Al or 6061 cold spray coatings causes a moderate increase in the hardness of the coating, the wear rate of the coatings is very low compared to the bulk alloys examined, provided the Al_2O_3 content is above a critical level. Specifically, a wear reduction in wear rate between 3 and 5 decades is observed when the composite cold spray coatings are compared with bulk Al–12 wt.%Si, 356.0 Al and AZ91E T6.
4. Increasing Al_2O_3 additions to the coating gradually changes the wear mode from adhesive to abrasive. This change in wear mode is accompanied by an increased but more stable friction coefficient. Once the wear mode becomes fully abrasive the wear rate is reduced by several orders of magnitude. The transition in wear mode occurs with a much lower Al_2O_3 content for the 6061 alloy based composite coatings than that for pure Al-based coatings.

Acknowledgements

Funding for this project through the Australian Research Council Centre of Excellence for Design in Light Metals is gratefully acknowledged.

References

[1] A.A. Luo, A.K. Sachdev, Wrought Magnesium Research for Automotive Applications, in: A.A. Luo, N.R. Neelameggham, R.S. Beals (Eds.), Magnesium Technology, vol. 2006, TMS (The Minerals, Metals and Materials Society), San Antonio, TX, USA, 2006, p. 333.
[2] J. Abthoff, W. Gelse, J. Lang, Magnesium Alloys and Their Application as Housing Material for Sports Prototype and Passenger Cars, in: G.W. Lorimer (Ed.), 3rd International Magnesium Conference, The Institute of Materials, Manchester, UK, 1997, p. 193.
[3] D.A. Gerard, Adv. Mater. Processes 166 (2008) 30.
[4] G. Song, A. Atrens, Adv. Eng. Mater. 9 (2007) 177.
[5] G. Song, A. Atrens, M. Dargusch, Corros. Sci. 41 (1999) 249.
[6] J. An, R.G. Li, C.M. Chen, Y. Xu, X. Chen, Z.X. Guo, Y.B. Liu, Mater. Sci. Technol. 23 (2007) 1208.
[7] B. Luan, J.E. Gray, J. Alloys Compd. 336 (2002) 88.
[8] M. Parco, L. Zhao, J. Zwick, K. Bobzin, E. Lugscheider, Surf. Coat. Technol. 201 (2006) 3269.
[9] A. Pardo, M.C. Merino, M. Mohedano, P. Casajús, A.E. Coy, R. Arrabal, Surf. Coat. Technol. 203 (2009) 1252.
[10] H. Pokhmurska, B. Wielage, T. Lampke, T. Grund, M. Student, N. Chervinska, Surf. Coat. Technol. 202 (2008) 4515.
[11] Z. Wei, L. Liu, W. Ding, Mater. Sci. Forum 488–489 (2005) 685.
[12] V.K. Champagne Jr (Ed.), The Cold Spray Materials Deposition Process, Woodhead Publishing, Cambridge, 2007.
[13] Papyrin; A. N., USA, Patent #5304414, 1994.
[14] E. Irissou, J.-G. Legoux, B. Arsenault, C. Moreau, J. Therm. Spray Technol. 16 (2007) 661.
[15] E. Sansoucy, P. Marcoux, L. Ajdelsztajn, B. Jodoin, Surf. Coat. Technol. 202 (2008) 3988.
[16] W.Y. Li, G. Zhang, H.L. Liao, C. Coddet, J. Mater. Process. Technol. 202 (2008) 508.
[17] K. Spencer, M.-X. Zhang, Key Eng. Mater. 384 (2008) 61.
[18] E. Irissou, J.-G. Legoux, A. Ryabinin, B. Jodoin, C. Moreau, J. Therm. Spray Technol. 17 (2008) 495.
[19] C.H. Caceres, Mater. Sci. Forum 519–521 (2006) 1801.
[20] J. Karthikeyan, Adv. Mater. Processes 164 (2006) 12.
[21] H. Gabel, Adv. Mater. Processes 162 (2004) 47.
[22] I.L. Rozenfel'd, V.P. Persiantseva, V.E. Zorina, Protection of Metals 15 (1979) 69.
[23] K. Spencer, M.X. Zhang, Scripta Mater. 61 (2009) 44.
[24] W. Han, E.F. Rybicki, J.R. Shadley, J. Therm. Spray Technol. 2 (1993) 145.
[25] V.K. Pecharsky, P.Y. Zavalij, Fundamentals of Powder Diffraction and Structural Characterization of Materials, 2005, Springer, New York, 2005, p. 360.
[26] EVA 13 User Manual, Release 2007, Bruker AXS GmbH, Karlsruhe, Germany, 2007.
[27] Z. Szklarska-Smialowska, Corros. Sci. 41 (1999) 1743.
[28] W.-Y. Li, C.-J. Li, H. Liao, J. Therm. Spray Technol. 15 (2006) 206.
[29] T. Stoltenhoff, C. Borchers, F. Gartner, H. Kreye, Surf. Coat. Technol. 200 (2006) 4947.
[30] E. Calla, D. McCartney, P. Shipway, J. Therm. Spray Technol. 15 (2006) 255.
[31] W.B. Choi, L. Li, V. Luzin, R. Neiser, T. Gnaupel-Herold, H.J. Prask, S. Sampath, A. Gouldstone, Acta Mater. 55 (2007) 857.
[32] F. Gartner, T. Stoltenhoff, J. Voyer, H. Kreye, S. Riekehr, M. Kocak, Surf. Coat. Technol. 200 (2006) 6770.
[33] A. Hall, D. Cook, R. Neiser, T. Roemer, D. Hirschfeld, J. Therm. Spray Technol. 15 (2006) 233.
[34] H. Koivuluoto, J. Lagerbom, P. Vuoristo, J. Therm. Spray Technol. 16 (2007) 488.
[35] W.Y. Li, X.P. Guo, C. Verdy, L. Dembinski, H.L. Liao, C. Coddet, Scripta Mater. 55 (2006) 327.
[36] Y.L. Shen, J.J. Williams, G. Piotrowski, N. Chawla, Y.L. Guo, Acta Mater. 49 (2001) 3219.
[37] D. Teirlinck, F. Zok, J.D. Embury, M.F. Ashby, Acta Metall. 36 (1988) 1213.
[38] J.R. Rice, D.M. Tracey, J. Mech. Phys. Solids 17 (1969) 201.
[39] P.J. Blau, Friction and Wear Transitions of Materials, Noyes Publications, Park Ridge, New Jersey, USA, 1989.
[40] A.T. Alpas, J.D. Embury, Scripta Metall. Mater. 24 (1990) 931.
[41] A.P. Sannino, H.J. Rack, Wear 189 (1995) 1.
[42] A. Alpas, J. Zhang, Metall. Mater. Trans. A 25 (1994) 969.
[43] E. Rabinowicz, Determination of the compatibility of metals through static friction tests, ASLE Transactions, vol. 14, 1971, p. 198.
[44] E. Rabinowicz, Friction and Wear of Materials, 2nd Ed.John Wiley & Sons, New York, 1995.
[45] D.H. Buckley, J. Coll. Interf. Sci. 58 (1977) 36.
[46] P.J. Alison, H. Wilman, Br. J. Appl. Phys. 15 (1964) 281.
[47] G.V. Raynor, The Physical Metallurgy of Magnesium and its Alloys, Pergamon, New York, 1959.
[48] H. Chen, A.T. Alpas, Wear 246 (2000) 106.
[49] D.H. Buckley, R.L. Johnson, ASLE Trans. 9 (1966) 121.